Appl Nanosci (2015) 5:937–944
DOI 10.1007/s13204-014-0397-z

ORIGINAL ARTICLE

Biosynthesis of silver nanoparticles from *Premna serratifolia* L. leaf and its anticancer activity in CCl_4-induced hepato-cancerous Swiss albino mice

J. Arockia John Paul · B. Karunai Selvi · N. Karmegam

Received: 19 November 2014 / Accepted: 24 December 2014 / Published online: 7 January 2015

Abstract In this study, we report the biosynthesis of silver nanoparticles using the ethanolic leaf powder extract of *Premna serratifolia* L. and its anticancer activity in carbon tetra chloride (CCl_4)-induced liver cancer in Swiss albino mice (Balb/c). The synthesized silver nanoparticles were characterized by SEM, FTIR and XRD analyses. The Debye–Scherrer equation was used to calculate particle size and the average size of silver nanoparticles synthesized from *P. serratifolia* leaf extract was 22.97 nm. The typical pattern revealed that the sample contained cubic structure of silver nanoparticles. FTIR analysis confirmed that the bioreduction of silver ions to silver nanoparticles is due to reduction by capping material of the plant extract. The silver nanoparticles of *P. serratifolia* leaf extract were effective in treating liver cancer in Swiss albino mice when compared with *P. serratifolia* leaf extract with isoleucine.

Keywords Anticancer activity · Bioreduction · Liver cancer · *Premna serratifolia* · Silver nanoparticles

J. Arockia John Paul (✉)
Department of Zoology, Arumugam Pillai Seethai Ammal College, Tiruppattur 630 211, Tamil Nadu, India
e-mail: jajpaul@gmail.com

B. Karunai Selvi
Department of Botany, V.V. Vanniaperumal College for Women, Virudhunagar 626 001, Tamil Nadu, India

N. Karmegam
Department of Botany, Government Arts College, Salem 636 007, Tamil Nadu, India

Introduction

Nanotechnology involves the production, manipulation and use of materials ranging in size from less than a micron to that of individual atoms. A wide variety of physical, chemical and biological process results in synthesis of nanoparticles, some of these are novel and others are quite common (Sastry et al. 2004). The use of environmentally benign materials like plant components, bacteria and fungi for the synthesis of silver nanoparticles (AgNps) offers numerous benefits and is compatible for pharmaceutical and biomedical applications (Parashar et al. 2009).

The use of plants for fabrication of AgNps has drawn the attention of researchers as it is rapid, low-cost and single-step method for the biosynthesis process. The rate of reduction of metal ions using plants has been found to be much faster as compared to microorganisms and in stable formation of metal nanoparticles (Rai et al. 2008). The shape and size of nanoparticles synthesized from plants can be controlled and modulated by changing the pH. The biosynthetic method employing plant extracts has received attention as being simple and viable compared to chemical and physical methods for synthesizing metal nanoparticles (Torresdey et al. 2003).

The formation of AgNps using plants can be visually observed due to the yellowish brown coloration of the extract and can be further confirmed by spectroscopic methods. The synthesis of AgNps using different plant species, *Medicago sativa* (Torresdey et al. 2003), *Cinnamomum camphora* (Huang et al. 2007), *Diospyros kaki* (Song and Kim 2008), *Coriandrum sativum* (Sathyavathi et al. 2010), *Lippia nodiflora* (Paul et al. 2013) has been reported. AgNps were synthesized using *Euphorbia hirta* and *Nerium indicum* plant extract and applied for bactericidal activity (Mano Priya et al. 2011).

The plant selected for the present study, *Premna serratifolia* L., is widely distributed along the coasts and islands of tropical and subtropical Asia, Africa, Australia and the Pacific and has been reported for antioxidant and tumor cell suppression potential in three different cancer cell lines MCF7 (breast cancer), HepG2 (liver cancer) and A549 (lung cancer) by SRB assay (Selvam et al. 2012). *P. serratifolia* is selected based on the local availability, medicinal uses and its significant metabolites (Basu and Dandiya 2006; Singh et al. 2011). However, the research on the biosynthesized AgNps from *P. serratifolia* leaves for anticancer activity is hitherto unavailable. Hence, the present study has been carried out to biosynthesize AgNps using leaf powder extract of *P. serratifolia* and to study its anticancer activity using mice model.

Materials and methods

Collection of plant materials and extraction

The plant material was collected from Megamalai, Varusanadu Hills, Theni District, Tamil Nadu and authenticated by the Rapinat Herbarium, Tiruchirappalli, Tamil Nadu, India. The leaves of *P. serratifolia* were washed thoroughly with double distilled water and dried in air and then milled to fine powder. The dried and powdered plant materials (100 g) were extracted successively with 600 ml of ethanol (1:6 w/v) using soxhlet extractor for 48 h at a temperature not exceeding the boiling point of the solvent (Lin et al. 1999). The extracts were filtered using Whatman No.1 filter paper and then concentrated in vacuum at 40 °C using a rotary evaporator. The extract was stored at 4 °C for further experiments.

Biosynthesis of AgNps

Aqueous solution of 1 mM silver nitrate ($AgNo_3$) was prepared and used for the synthesis of AgNps. Five ml of ethanolic leaf extract was added to vigorously stirred 25 ml of aqueous solution of 1 mM silver nitrate for reduction into silver ions and kept at room temperature. After 10 min, the change of the color was noted from colorless to yellowish brown indicating the formation of AgNps (Jain et al. 2009).

UV–visible absorbance spectroscopy analysis

The reduction of pure Ag^+ ions was monitored by measuring the UV–visible spectrum of the reaction mixture at various time intervals, i.e., 10, 30, 60 and 120 min. It was filtered by Whatman No.1 filter paper. The filtrate was subjected to UV–Vis spectral analysis using a Perkin-Elmer Lambda 25 Spectrophotometer. The peak shifted in the absorption spectrum from 340 to 620 nm with increasing reaction time was observed.

SEM analysis

SEM analysis was done using Hitachi S-4500 SEM machine. Thin film of the sample were prepared on a carbon-coated copper grid by just dropping a very small amount of the sample on the grid, extra solution was removed using a blotting paper and then the film on the SEM grid was allowed to dry by putting it under a mercury lamp for 5 min (Jain et al. 2009).

FTIR spectroscopy analysis

To remove any free biomass residue (or) compound that is not the copping ligand of the nanoparticles, the residual solution of 100 ml after reaction was centrifuged at 15,000 rpm for 15 min and the resulting suspension was redispersed in 10 ml sterile deionized water. The centrifuging and redispersing process was repeated three times. Thereafter, the purified suspension was freeze dried to obtain dried powder. Finally, the dried nanoparticles were analyzed by FTIR Nicolet Avatar-660 Machine.

XRD analysis

AgNp solution thus obtained was purified by repeated centrifugation at 10,000 rpm for 10 min followed by redispersion of the pellet of AgNps into deionized water for 10 min. After freeze drying, the structure, size and composition of the silver particles were analyzed by X-Ray diffraction studies (Jain et al. 2009). It was operated at a voltage of 40 kV and a current of 30 mA with CuKα radiations in 2θ configurations. The crystallite domain size was calculated from the width of the XRD peaks, assuming that they are free from non-uniform strains using the Debye–Scherrer formula:

$$D = 0.94\,\lambda/\beta\cos\theta$$

where D is the average crystallite domain size, perpendicular to the reflecting planes; λ is the X-ray wavelength; β is the full width at half maximum and θ is the diffraction angle.

Anticancer activity of leaf extract and AgNps of *P. serratifolia*

Experimental animals

Male Swiss albino mice (Balb/c) weighing 25 ± 3 g were used for the study. Mice were maintained under standard

environmental condition (temperature 27 ± 2 °C and 12 h light/dark cycle) and they were allowed with standard laboratory feed and water ad libitum. Initial body weights of all animals were recorded. Ethical clearance for the use of animals was obtained from the committee constituted in Sri Kaliswari College, Sivakasi for the purpose (Regn. No. 1086/AC/07/CPCSEA).

Experimental design

A total of 30 albino mice were divided into 5 groups of 6 animals each to evaluate the anticancer activity of synthesized silver nanoparticles. Group I: normal control mice (healthy mice); Group II: animals were treated with intraperitoneal injection of 50 % CCl_4 in olive oil twice a week for 6 weeks to induce liver cancer; Group III: liver cancer induced mice treated with *P. serratifolia* leaf extract (500 mg/Kg) for 15 days; Group IV: liver cancer induced mice treated with synthesized AgNps coated with *P. serratifolia* leaf extract (500 mg/Kg) for 15 days; Group V: liver cancer induced mice treated with standard amino acid, isoleucine (3 g/d) for 15 days. After the experimental duration, blood serum and plasma samples from control and cancer induced animals were collected for biochemical analysis.

Biochemical estimation

Estimation of SGOT and SGPT was based on the reference method described by Reitmann and Frankel (1957). The SGOT and SGPT were measured at 540 nm and expressed as IU/ml. Lowry's method (Lowry et al. 1951) was followed for the estimation of total protein. Serum was mixed with alkaline copper sulfate solution and Folin–ciocalteu reagent and incubated for 30 min and the blue color developed was measured at 650 nm and expressed as µg/ml. Plasma thiobarbituric acid-reactive substances (TBARS) were estimated by Yagi's method (1978), measured at 530 nm and expressed as nmol/ml. 1,1-Diphenyl-2-picrul-hydrazil free radical (DPPH) and hydrogen peroxide scavenging effects were studied using the method of Blois (1958) and Rajan et al. (2011).

The capacity to scavenge the DPPH radical was calculated using the following equations. The percent inhibition was calculated as:

$$\text{Percent DPPH scavenging activity} = (A\ \text{control} - A\ \text{test})/A\ \text{control} \times 100$$

where A control is the absorbance of the control reaction and A test is the absorbance of the extract. The antioxidant activity of the extract was expressed as IC 50. The IC 50 value was defined as the concentration in µg/ml of extract that inhibits the formation of DPPH radical by percent.

The extent of H_2O_2 scavenging of the plant extracts was calculated as:

$$\text{Percent scavenging of hydrogen peroxide} = \frac{(A0 - A1) \times 100}{A0}$$

$A0$ = Absorbance of control $A1$ = Absorbance in the presence of plant extract.

The statistical difference of the above parameters between the treatments was carried out by ANOVA.

Results and discussion

The synthesized AgNps were detected by change of color from colorless to yellowish brown by using UV–Vis spectrophotometer at various nm (Fig. 1). Absorption spectra of AgNps were formed in the reaction mixture at different time intervals: 10, 30, 60 and 120 min and at various nm: 340, 380, 420, 460, 500, 540, 580 and 620. A strong absorption band with a maximum absorbance at 460 nm was observed. Narayanan and Sakthivel (2011) obtained 457 nm in UV–Vis absorption spectroscopy while analyzing the fungal mycelia treated with $AgNO_3$ and confirmed the formation of AgNps. As the leaf extract was mixed with the aqueous solution of the silver ion complex, it started changing from colorless to yellowish brown color due to the excitation of surface plasmon vibrations indicating the formation of AgNps. UV–Vis spectroscopy is well known to investigate shape and size controlled of nanoparticles. In the present study, the UV–Vis spectrograph of the colloid of the AgNps has been recorded as a function of time by using a quartz cuvette with silver nitrate as the reference (Jain et al. 2009). In *P. serratifolia* leaf powder extract, the broadening of peak indicated that the particles are polydispersed. This peak has been assigned to a surface plasmon phenomenon, i.e., well-documented for various metal nanoparticles with a size range between 25 and 100 nm (Sastry et al. 2004). The position and shape of the plasma absorption depend on the particle size, shape and dielectric constant of the surrounding medium (Guzman et al. 2008). The reduction of silver ions and the formation of stable nanoparticles occurred rapidly within 1 h of reaction, making it one of the fastest bioreducing methods to produce silver nanostructure (Sathyavathi et al. 2010).

The SEM image confirmed the presence of high-density AgNps synthesized by *P. serratifolia* leaf extract (Fig. 2). The SEM analysis revealed the particle size between 15 and 100 nm as well as the cubic structure of the AgNps. The SEM analysis showed that the AgNps were partially aggregated. In Fig. 2, silver nanoparticles were found within the aggregates excepting few. The nanoparticles

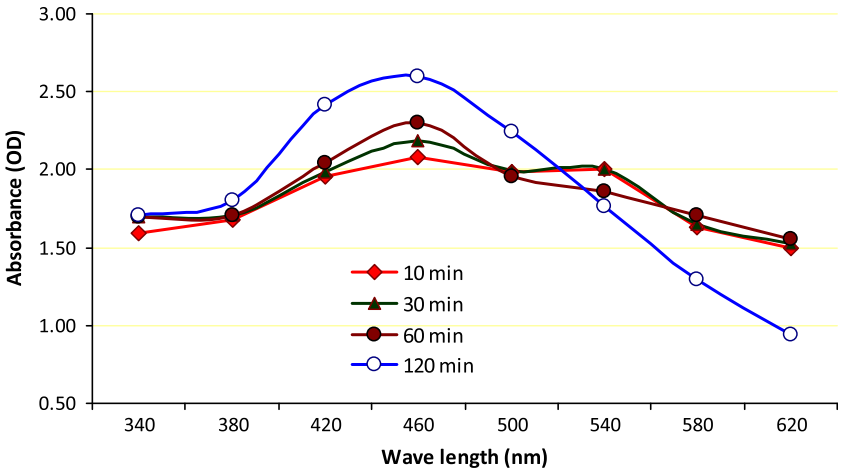

Fig. 1 Optical density of silver nanoparticles synthesized using *P. serratifolia* leaf extract

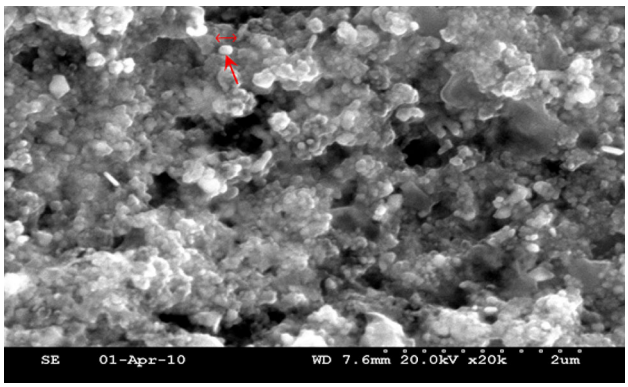

Fig. 2 SEM micrograph of silver nanoparticles synthesized using *P. serratifolia* leaf extract (Particle shown by *red arrow*)

were not in direct contact even within the aggregates, indicating stabilization of the nanoparticles by a capping agent (Song and Kim 2008).

FTIR spectrum of aqueous AgNps synthesized from *P. serratifolia* leaf extract is shown in Fig. 3. The peaks near 3,441, 2,924 and 2,854 cm^{-1} were found to match OH stretching and aldehydic C–H stretching. The weaker bond at 1,629 cm^{-1} was corresponding to amide 1, arising due to carbonyl stretching proteins. The peak at 1,041 cm^{-1} was corresponding to C–N stretching vibration of the amine. The peak near 1,741 cm^{-1} was corresponding to C=C stretching (non-conjugated). The peak at 1,383 cm^{-1} was corresponding to C–H bending ($–CH_3$). The peak near 833 cm^{-1} was matching to $–C=CH_2$. The peaks at 677 and 652 cm^{-1} were found to correspond CH out-of-plane bending vibrations which was substituted by ethylenic systems –CH=CH– (cis). FTIR analysis confirmed that the bioreduction of silver ions to AgNps is due to the reduction by capping material of the plant extract. The amide linkages between amino acid residues in proteins give rise to the well-known signatures in the infrared region of the electromagnetic spectrum. The overall observation confirms the presence of protein in the samples of silver nanoparticles. It is reported earlier that proteins can bind to nanoparticles either through free amine groups or cysteine residues in the proteins (Kittel 1992; Gole et al. 2001). IR spectroscopic study confirmed that the carbonyl group from amino acid residue and proteins has the strongest ability to bind metal indicating the proteins could possibly form a layer covering the metal nanoparticles (i.e., capping of AgNps) to prevent agglomeration and thereby stabilize the medium. This suggests that the biological molecules could possibly perform the dual functions of formation and stabilization of AgNps in the aqueous medium (Sathyavathi et al. 2010). The absorption peak at 1,635 cm^{-1} is close to that reported for native proteins (Macdonald and Smith 1996) which suggest that proteins are interacting with biosynthesized nanoparticles and also their secondary structure was not affected during reaction with Ag ions or after binding with Ag nanoparticles (Fayaz et al. 2010). These IR spectroscopic studies confirmed that carbonyl group of amino acid residues have strong binding ability with metal suggesting the formation of layer covering metal nanoparticles and acting as capping agent to prevent agglomeration and providing stability to the medium (Sathyavathi et al. 2010). These results confirm the presence of possible proteins acting as reducing and stabilizing agents for silver nanoparticles.

The biosynthesis of AgNps using *P. serratifolia* leaf powder extract was further confirmed by XRD image (Fig. 4). The XRD pattern showed several peaks with four intense peaks in the whole spectrum of 2θ values ranging from 33 to 77 (Table 1). XRD spectra of pure crystalline silver structures have been published by the Joint Committee on Powder Diffraction Standards (file no. 04-0783). A comparison of our XRD spectrum with the standard confirmed that the silver particles formed in the present experiments were in the form of nanocrystals, as evidenced by the diffractions of peaks at 2θ values of 38.45°, 44.48°,

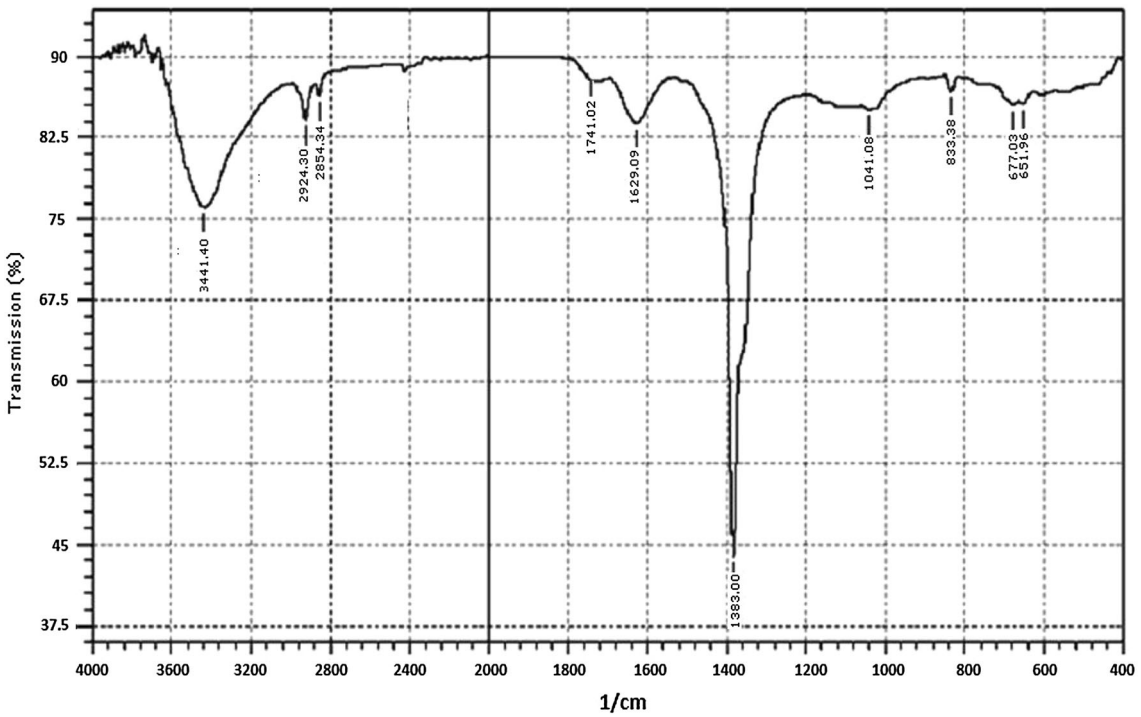

Fig. 3 FTIR spectrum of silver nanoparticles synthesized using *P. serratifolia* leaf extract

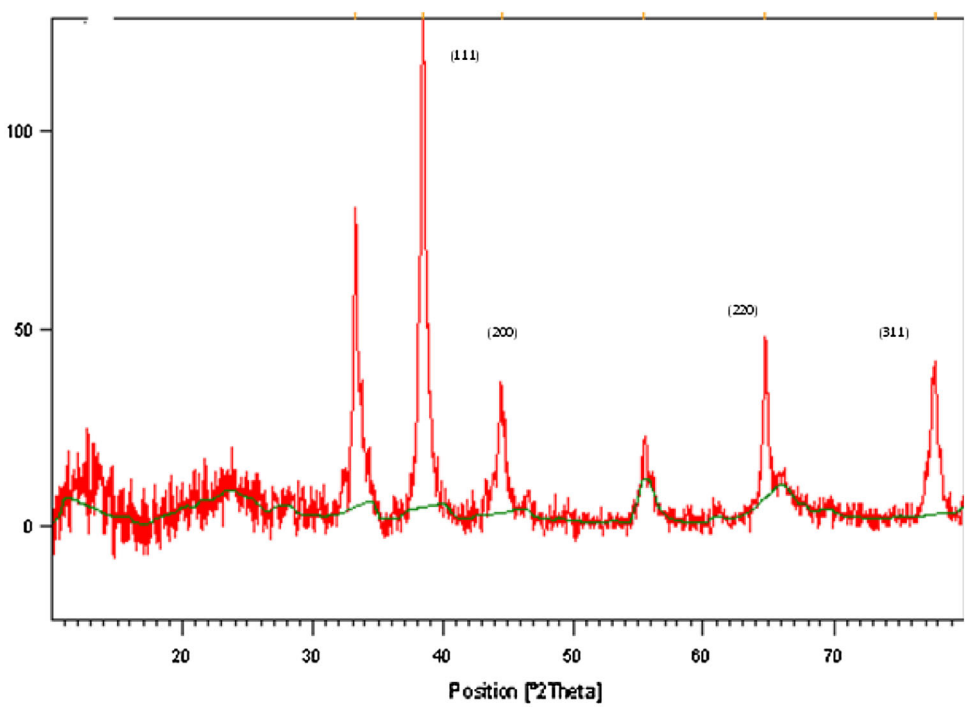

Fig. 4 XRD pattern of silver nanoparticles synthesized using *P. serratifolia* leaf extract

64.69° and 77.62°, corresponding to 111, 200, 220, and 311 planes of the face-centered cubic (fcc) for silver, respectively. This is in agreement with the results obtained by other workers (Martinez-Castanon et al. 2008; Parikh et al. 2011; Theivasanthi and Alagar 2011). Moreover, few small insignificant impurity peaks were also observed, which may be attributed to other organic substances in reaction mixture. The full width at half maximum (FWHM) values measured for 111, 200, 220, and 311 planes of reflection were used with the Debye–Scherrer equation to calculate

Table 1 Size of silver nanoparticles synthesized using *P. serratifolia* leaf extract

Pos. (°2Th.)	Height (cts)	FWHM (°2Th.)	d-spacing (Å)	Rel. Int. (%)	Particle size in nm
33.2663	74.78	0.2676	2.69330	61.78	32.39
38.4554	121.04	0.4015	2.33975	100.00	21.90
44.4811	26.99	0.5353	2.03407	22.30	16.76
55.3815	4.11	0.3610	1.65900	3.40	25.97
64.6916	36.05	0.4015	1.44093	29.78	24.48
77.6293	36.45	0.6528	1.22798	30.11	16.33
Average size of the nanoparticles					22.97

the size of the nanoparticles. Average size of the particles synthesized was 22.97 nm with a size range between 16 and 32 nm.

The XRD pattern of the silver nitrate-treated sample corresponds to that of silver nanoparticles. It is important to know the exact nature of the silver particles formed and this can be deduced from the XRD spectrum of the sample. The typical XRD pattern revealed that the sample contains cubic structure of AgNps. The broadening of Bragg peaks is primarily due to the formation of small particle size of silver. The lattice constant calculated from this pattern was 4.0892A°, a value in agreement with the literature report ($a = 4.086$A°, Joint Committee on Powder Diffraction Standards file no. 04-0783). The result reveals that the Ag^+ of silver nitrate had indeed been reduced to Ag^0 by this extract under the reaction conditions.

Table 2 shows that the body mass, SGOT, SGPT, total protein and plasma TBARS level of control and liver cancerous mice. The body mass of mice was decreased after the liver cancer was developed. After that, the mice treated with *P. serratifolia* leaf extract and isoleucine amino acid regained its body mass. When compared with plant extract and amino acid treated mice, AgNps coated with *P. serratifolia* leaf extract treated mice regained the body mass more near to control. The level of SGOT, SGPT and total protein in experimental mice in each group was significantly increased in CCl_4-induced liver cancerous mice when compared to control groups. The treatment of AgNps of *P. serratifolia* powder extract significantly restrained the level of SGOT, SGPT and total protein as normal near to control in comparison to liver cancer mice treated with *P. serratifolia* leaf powder extract + isoleucine. There was a significant decrease in plasma TBARS level in CCl_4-induced liver cancerous mice when compared to control groups. The treatment of AgNps coated with *P. serratifolia* leaf extract significantly restrained the level of plasma TBARS as normal near to control when compared to liver cancerous mice treated with *P. serratifolia* leaf extract + isoleucine.

The use of nanotechnology in medicine offers some exciting possibilities. When compared with normal mice, CCl_4-treated mice possess increased level of SGOT, SGPT, total protein and decreased plasma TBARS, where recovery of these parameters to normal level was found significant in AgNps of *P. serratifolia* leaf powder extract than *P. serratifolia* leaf powder extract + isoleucine treatment groups. Similar observation was made (Mandal et al. 2005; Jeyachandran et al. 2007) while studying the anticancer activity of *Anisomeles malabarica* and *Solidago microglossa*, respectively. In the present study, it was observed that the animals treated with CCl_4 resulted in the significant hepatic damage as shown by the elevated levels of marker enzymes. These changes in the marker level will reflect in hepatic structural integrity. The rise in the SGPT plays a vital role in the conversion of alanine to pyruvate and glutamate (amino acids to ketoacid) (Singh et al. 2011). The normalization of the serum markers by the extract-coated nanoparticles suggests that they are able to condition the hepatocytes so as to protect the membrane integrity against CCl_4-induced leakage of marker enzymes in the circulation. The above changes can be considered as an expression of the functional improvement of hepatocytes, which may be caused by an accelerated regeneration of parenchyma cells (Jain et al. 2009).

Table 2 Effect of silver nanoparticles synthesized from *P. serratifolia* leaf on biochemical parameters of CCl_4-induced liver cancerous Swiss albino mice (values are mean ± SD)

Groups	Treatments	Body mass (gm)	SGOT (IU ml^{-1})	SGPT (IU ml^{-1})	Total protein (μg/ml)	Plasma TBARS (nmol/ml)
I	Control	26.78 ± 1.12	223.18 ± 14.33	184.25 ± 8.66	113 ± 2.16	111.84 ± 6.33
II	CCl_4 + olive oil	18.91 ± 0.85c	375.45 ± 21.00a	607.54 ± 41.33a	218 ± 7.54a	69.76 ± 4.00a
III	CCl_4 + olive oil +*P. serratifolia* leaf extract	22.89 ± 1.05	289.54 ± 13.33b	245.28 ± 16.00a	145 ± 4.00a	92.60 ± 5.33c
IV	CCl_4 + olive oil + *P. serratifolia extract*-coated AgNp's	25.47 ± 1.76c	249.48 ± 11.66a	219.27 ± 15.66a	124 ± 6.85a	102.55 ± 6.66b
V	CCl_4 + olive oil + Isoleucine	23.95 ± 1.43	267.81 ± 14.66a	238.37 ± 12.33a	139 ± 8.75a	96.39 ± 3.66c

One-way ANOVA *P* values are significantly different at a < 0.001; b < 0.01; c < 0.005; Group II compared with Group I and Groups III, IV and Group V compared with Group II

Table 3 Effect of *P. serratifolia* leaf extract on DPPH and H_2O_2 assay (values are mean ± SD)

Concentration of *P. serratifolia* leaf extract (μg/ml)	% of antioxidant activity in DPPH assay	% of inhibition in H_2O_2 assay
200	38.0 ± 1.00	52.54 ± 0.69
400	54.7 ± 2.66	56.00 ± 1.02
600	59.8 ± 4.00	61.53 ± 2.15
800	68.9 ± 4.33	63.61 ± 3.92
1,000	73.5 ± 4.66	69.24 ± 3.97

The results of antioxidant and radical scavenging activity of *P. serratifolia* leaf powder extract are given in Table 3. The extract (1,000 μg) exhibited 73.5 ± 4.66 and 69.24 ± 3.97 % of antioxidant and H_2O_2 radical scavenging activity, respectively, which revealed that the leaves of *P. serratifolia* possess the anticancer activity and radical scavenging activity. *Euphorbia neriifolia* extract significantly restored the antioxidant enzyme level in the liver and exhibited significant dose-dependant protective effect against DENA-induced liver toxicity, which can be mainly attributed to the antioxidant property of the extract (Sabir et al. 2012). AgNps synthesized using *Alternanthera sessilis* (Linn.) extract showed antimicrobial and antioxidant activities (Pracheta et al. 2011). AgNps biosynthesized from ethanolic extracts of *Phytolacca decandra*, *Gelsemium sempervirens*, *Hydrastis canadensis* and *Thuja occidentalis* showed differences in their level of anticancer and antibacterial potentials (Niraimathi et al. 2013). Presence of more alkaloids (Alam et al. 1993) and flavonoids (Singh et al. 2011) was reported from *P. serratifolia.* The anticancer activity may be due to the presence of flavonoids in the plant extract.

Hepatotoxic effect of carbon tetrachloride is due to oxidative damage by free radical generation and antioxidant property is claimed to be one of the mechanisms of hepatoprotective drugs. The preliminary phytochemical reports of *P. serratifolia* revealed that the ethanolic extract of the leaves was found to contain higher concentration of flavonoids and alkaloids. It has been reported that the flavonoid possess antioxidant properties by free radical scavenging. Flavonoids are phenolic compounds widely distributed in plants, which have been reported to exert multiple biological effects, including antioxidant and free radical scavenging abilities (Alam et al. 1993).

Conclusions

Average size of AgNps synthesized was 22.97 nm with the size range between 16 and 32 nm. The spectroscopic techniques (FT-IR and UV–Vis) including morphological (SEM) and structural (XRD) studies suggest that the protein might have played an important role in the stabilization of silver nanoparticles through coating of protein moiety on the silver nanoparticles. In the present study, we have confirmed that the anticancer activities of AgNps of *P. serratifolia* leaf powder extract in CCl_4-induced liver cancer. The AgNps of *P. serratifolia* have been proven for their non-toxic and protective effects over the organs without including any lethal effects in the mice model, thereby accomplishing a sustained control over the disease progression. These potential applications of AgNps of *P. serratifolia* in preventing the effects, induced at cancerous condition, have opened up way for a new resource of cost-economic alternative in the treatment of cancer progression. Our further aim is to understand the biochemical and molecular mechanism of restraining the level of biochemical parameters by treatment of synthesized silver nanoparticles of *P. serratifolia.*

Acknowledgments The authors gratefully acknowledge the Central Electrochemical Research Institute, Karaikudi, Tamil Nadu for their help in SEM and XRD analyses.

References

Alam M, Rukmani B, Meenakshi N, Dasan KS, Bhima RR (1993) Standardization studies of some dasamula containing formulations. J Res Ayur Siddha 4:68–73

Basu NK, Dandiya PC (2006) Chemical investigation of *Premna integrifolia* Linn. J Am Pharm Assoc 36:389–391

Blois MS (1958) Antioxidant determinations by the use of a stable free radical. Nature 181:1198–1200

Fayaz AM, Balaji K, Girilal M, Yadav R, Kalaichelvan PT, Venketesan R (2010) Biogenic synthesis of silver nano-particles and their synergistic effect with antibiotics: a study against Gram-positive and Gram-negative bacteria. Nanomed Nanotechnol Biol Med 6:103–109

Gole A, Dash C, Ramachandran V, Sainkar SR, Mandale AB, Rao M, Sastry M (2001) Pepsin − gold colloid conjugates: preparation, characterization, and enzymatic activity. Langmuir 17:1674–1679

Guzman MG, Dille J, Godet S (2008) Synthesis of silver nanoparticles by chemical reduction method and their antibacterial activity. World Acad Sci Engg Technol 43:357–363

Huang J, Chen C, Hong J, Qingbiaco L, Shao W, Sun D, Wang XH, Xang X (2007) Biosynthesis of silver and gold nanoparticles by novel sun dried *Cinnamomum camphora* leaf. Nanotechnol 18:105–106

Jain D, Daima HK, Kachiwaha S, Kotheri SL (2009) Synthesis of plant mediated silver nanoparticles using papaya fruit extract and evolution of their antimicrobial activities. Dig J Nanomater Biostruct 4:557–563

Jeyachandran R, Mahesh A, Cindrella L (2007) DEN-induced cancer and its alleviation by *Anisomeles malabarica* (L.) R.Br. ethanolic leaf extract in male albino mice. Int J Cancer Res 3:174–179

Kittel C (1992) Introduction to Solid State Physics. Wiley Eastern Limited, India

Lin J, Opak WAR, Keller MG (1999) Preliminary screening of some traditional zulu medicinal plants for anti-inflammatory and anti-microbial activities. J Ethnopharmacol 68:267–274

Lowry OH, Rosebrough MN, Farr AL, Randall RJ (1951) Protein measurement with folin's phenol reagent. J Biol Chem 193:265–275

Macdonald IDG, Smith WE (1996) Orientation of cytochrome C adsorbed on a citrate-reduced silver colloid surface. Langmuir 12:706–713

Mandal S, Phadtare S, Sastry M (2005) Interfacing biology with nanoparticles. Curr Appl Phys 5:118–127

Mano Priya M, Karunai Selvi B, Paul JAJ (2011) Green synthesis of silver nanoparticles from the leaf extracts of *Euphorbia hirta* and *Nerium indicum*. Dig J Nanomater Biostruct 6:869–877

Martinez-Castanon GA, Nino-Martinez N, Martinez-Gutierrez F, Martinez-Mendoza JR, Ruiz F (2008) Synthesis and antibacterial activity of silver nanoparticles with different sizes. J Nanopart Res 10(8):1343–1348

Narayanan KB, Sakthivel N (2011) Heterogeneous catalytic reduction of anthropogenic pollutant, 4-nitrophenol by silver-bionanocomposite using Cylindrocladium floridanum. Bioresour Technol 102:10737–10740

Niraimathi KL, Sudha V, Lavanya R, Brindha P (2013) Biosynthesis of silver nanoparticles using *Alternanthera sessilis* (Linn.) extract and their antimicrobial, antioxidant activities. Colloids Surf B 102:288–291

Parashar V, Sharma B, Pandey AC (2009) Parthenium leaf extract mediated synthesis of silver nanoparticles: a novel approach towards weed utilization. Dig J Nanomater Biostruct 4:45–50

Parikh RY, Ramanathan R, Coloe PJ, Bhargava SK, Patole MS, Shouche YS, Bansal V (2011) Genus-wide physicochemical evidence of extracellular crystalline silver nanoparticles biosynthesis by Morganella spp. PLoS One 6(6):e21401

Paul JAJ, Karunai Selvi B, Palanisamy AL (2013) Synthesis of silver nanoparticles from the leaf extract of selected plants. Nano Sci Nanotech Indian J 8:1–7

Pracheta VS, Paliwal R, Sharma S, Singh L, Janmeda BS, Savita SY, Sharma SH (2011) Chemoprotective activity of hydro-ethanolic extract of *Euphorbia neriifolia* Linn. leaves against DENA-induced liver carcinogenesis in mice. Biol Med 3:36–44

Rai M, Yadav A, Gade A (2008) CRC 675-Current trends in phytosynthesis of metal nanoparticles. Crit Rev Biotechnol 28:277–284

Rajan S, Mahalakshmi S, Deepa VM, Sathya K, Shajitha S, Thirunalasundari T (2011) Antioxidant potentials of *Punica granatum* fruit rind extracts. Int J Pharm Pharm Sci 3:82–88

Reitmann S, Frankel S (1957) Colorimetric estimation of serum GOT (glutamic oxaloacetic transaminase), GPT (glutamic pyruvate transaminase) activity. Am J Clini Pathol 28:56

Sabir SM, Ahmad SD, Hamid A, Khan MQ, Athayde ML, Santos DB, Boligon AA (2012) Antioxidant and hepatoprotective activity of ethanolic extract of leaves of *Solidago microglossa* containing polyphenolic compounds. Food Chem 131:741–747

Sastry M, Ahmad A, Khan MI, Kumar R (2004) Microbial nanoparticle production. In: Niemeyer CM, Mirkin CA (eds) Nanobiotechnology. Wiley-VCH, Weinheim, pp 126–135

Sathyavathi R, Balamurali Krishna M, Venugopal Rao S, Saritha R, Rao N (2010) Biosynthesis of silver nanoparticles using C*oriandrum sativum* leaf extract and their application in nonlinear optics. Adv Sci Lett 3:1–6

Selvam TN, Venkatakrishnan V, Damoder KS, Elumalai P (2012) Antioxidant and tumor cell suppression potential of *Premna serratifolia* Linn. leaf. Toxicol Int 19:31–34

Singh CRS, Nelson P, Muthukrishnan P, Mahesh K (2011) Hepatoprotective and anti-oxidant effect of root and root callus extract of *Premna serratifolia* L. in paracetamol induced liver damage in male albino rats. Int J Pharma Biosci 2:244–252

Song JY, Kim BS (2008) Biological synthesis of bimetallic Au/Ag nanoparticles using Persimmon (*Diospyros kaki)* leaf extract. Korean J Chem Engg 25:808–811

Theivasanthi T, Alagar M (2011) Electrolytic synthesis and characterizations of silver nanopowder. arXiv: 1111.0260

Torresdey JLG, Gombez G, Jose-Yaceman M, Parsons JG, Peralta-Videa JR, Tioani H (2003) Binding of silver (I) ions by Alfalfa biomass (*Medicago sativa*):batch pH, time, temperature and ionic strength studies. Hazard J Subst Res 4:1–15

Yagi K (1978) Lipid peroxides and human disease. Chem Physiol Lip 45:337–351